Dmbx1 is essential in agouti-related protein action

Wakako Fujimoto*†, Tetsuya Shiuchi‡, Takashi Miki*, Yasuhiko Minokoshi‡, Yoshihisa Takahashi*, Ayako Takeuchi*, Kazuhiro Kimura§, Masayuki Saito§, Toshihiko Iwanaga†, and Susumu Seino*¶

*Division of Cellular and Molecular Medicine, Kobe University Graduate School of Medicine, Kobe 650-0017, Japan; †Laboratory of Histology and Cytology, Graduate School of Medicine and §Laboratory of Biochemistry, Department of Biomedical Sciences, Graduate School of Veterinary Medicine, Hokkaido University, Sapporo 060-8638, Japan; and ‡Department of Developmental Physiology, National Institute for Physiological Sciences, Okazaki 444-8585, Japan

Edited by Richard D. Palmiter, University of Washington School of Medicine, Seattle, WA, and approved August 6, 2007 (received for review August 3, 2007)

Dmbx1 is a paired-class homeodomain transcription factor. We show here that mice deficient in *Dmbx1* exhibit severe leanness associated with hypophagia and hyperactivity and that isolation of a *Dmbx1*$^{-/-}$ mouse from its cohabitants induces self-starvation, sometimes leading to death, features similar to those of anorexia nervosa in humans. Interestingly, overexpression of agouti in *Dmbx1*$^{-/-}$ mice failed to induce aspects of the *A*^{y}*/a* phenotype, including hyperphagia, obesity, and diabetes mellitus. In *Dmbx1*$^{-/-}$ mice, administration of agouti-related protein increased cumulative food intake for the initial 6 h but significantly decreased it over 24- and 48-h periods. In addition, Dmbx1 was shown to be expressed at embryonic day 15.5 in the lateral parabrachial nucleus, the rostral nucleus of the tractus solitarius, the dorsal motor nucleus of the vagus, and the reticular nucleus in the brainstem, all of which receive melanocortin signaling, indicating involvement of Dmbx1 in the development of the neural network for the signaling. Thus, Dmbx1 is essential for various actions of agouti-related protein and plays a role in normal regulation of energy homeostasis and behavior.

A^{y}*/a* | feeding | leanness

The central nervous system is critical in the maintenance of energy homeostasis by regulating feeding and energy expenditure (1–3). In this regulation, the hypothalamus and brainstem play a central role by integrating peripheral signals (such as leptin) and central signals (including various neuropeptides). In normal individuals under negative energy balance, feeding is stimulated, and energy expenditure is decreased to prevent starvation. Conversely, under positive energy balance, feeding is suppressed, and energy expenditure is increased to prevent obesity. The former "starvation avoidance" system is more robust than the latter "obesity avoidance" system because survival is more acutely threatened by starvation than by obesity (3). Although these two systems interact, the starvation avoidance system works in principal through a pathway involving orexigenic neuropeptides such as agouti-related protein (AgRP) and neuropeptide Y (NPY), and the obesity avoidance system works in principal through anorexigenic neuropeptides, such as α-melanocyte stimulating hormone (α-MSH). AgRP, NPY, and α-MSH are abundantly expressed in the arcuate nucleus of the hypothalamus, which receives peripheral signals, such as leptin and ghrelin. Leptin reduces food intake and increases metabolic rate by activating proopiomelanocortin (POMC) gene expression (1–4) to increase the release of α-MSH, which activates downstream target neurons expressing melanocortin-3 receptors and melanocortin-4 receptors (MC4R) (5). By contrast, starvation or a decrease in fat mass stimulates food intake and suppresses metabolic rate by activating AgRP and NPY gene expression in arcuate neurons (1).

Loss-of-function mutations of *POMC* or *MC4R* lead to obesity associated with increased food intake and decreased energy expenditure in mice and humans (5). By contrast, mice with genetic disruption of AgRP and NPY exhibit only a modest metabolic phenotype with normal body weight, adiposity, and food intake (6), suggesting that NPY and AgRP are not essential in body weight regulation. Recently, however, by using temporally regulated ablation of AgRP neurons, AgRP neurons have been shown to be critical in the regulation (7–10). Furthermore, detailed analysis of AgRP knockout mice in older age indicates the importance of AgRP protein itself as well as of AgRP-bearing neurons (11).

By genetic disruption of mouse Dmbx1, a homeodomain transcriptional factor expressed at high levels in developing brain (12–16), we incidentally found that *Dmbx1* knockout (*Dmbx1*$^{-/-}$) mice exhibit severe leanness, abnormal feeding behavior, and hyperactivity. *Dmbx1*$^{-/-}$ mice were also generated by Ohtoshi *et al.* (17), whose work showed increased neonatal mortality and impaired growth. However, the mechanism underlying the phenotype in *Dmbx1*$^{-/-}$ mice has not yet been clarified.

Results

Severe Leanness of *Dmbx1*$^{-/-}$ Mice. *Dmbx1*$^{-/-}$ mice were indistinguishable from their littermates at birth. However, under normal breeding conditions, most *Dmbx1*$^{-/-}$ mice died before weaning. When the nonknockout (*Dmbx1*$^{+/+}$ and *Dmbx1*$^{+/-}$) littermates were removed from the cage before day 7, most *Dmbx1*$^{-/-}$ mice were able to survive until adolescence, but with body weight ≈30% less than that of *Dmbx1*$^{+/+}$ mice in both male mice (Fig. 1*A*) and female mice (data not shown). The body length of *Dmbx1*$^{-/-}$ mice as adults was >90% that of *Dmbx1*$^{+/+}$ mice (the nose–anal length of 16-wk-old male *Dmbx1*$^{+/+}$mice was 11.2 ± 0.1 cm, $n = 17$; that of male *Dmbx1*$^{-/-}$ mice was 10.4 ± 0.1 cm, $n = 16$). Histological examination of epididymal fat tissue revealed that the adipocytes of *Dmbx1*$^{-/-}$ mice were small in size [supporting information (SI) Fig. 6]. In addition, *Dmbx1*$^{-/-}$ mice showed low serum leptin levels (Fig. 1*B*). A decrease in fat mass results in a proportional reduction in serum leptin levels (18), so these data indicate that the fat mass is decreased in adult *Dmbx1*$^{-/-}$ mice.

Food Intake, Body Weight, and Locomotion Activity of *Dmbx1*$^{-/-}$ Mice. Female *Dmbx1*$^{+/+}$ and *Dmbx1*$^{-/-}$ mice were used for measuring food intake and body weight after isolation. The mice had been maintained in a group (four to six mice per cage) since birth and were housed individually at 20–24 wk of age. The body weight of *Dmbx1*$^{-/-}$ mice declined significantly more than the body weight

Author contributions: W.F., T.S., and T.M. contributed equally to this work; T.M., Y.M., and S.S. designed research; W.F., T.S., T.M., Y.M., Y.T., A.T., K.K., and T.I. performed research; T.S., Y.M., and M.S. contributed new reagents/analytic tools; W.F., T.M., Y.M., T.I., and S.S. analyzed data; and W.F., T.M., Y.M., and S.S. wrote the paper.

The authors declare no conflict of interest.

This article is a PNAS Direct Submission.

Freely available online through the PNAS open access option.

Abbreviations: AgRP, agouti-related protein; α-MSH, α-melanocyte stimulating hormone; E*n*, embryonic day *n*; i.c.v., intracerebroventricularly; MC4R, melanocortin-4 receptor; MT-II, melanotan-II; NTS, nucleus of the tractus solitarius; NPY, neuropeptide Y; POMC, proopiomelanocortin.

¶To whom correspondence should be addressed at: 7-5-1 Kusunoki-cho, Chuo-ku, Kobe 650-0017, Japan. E-mail: seino@med.kobe-u.ac.jp.

This article contains supporting information online at www.pnas.org/cgi/content/full/0707328104/DC1.

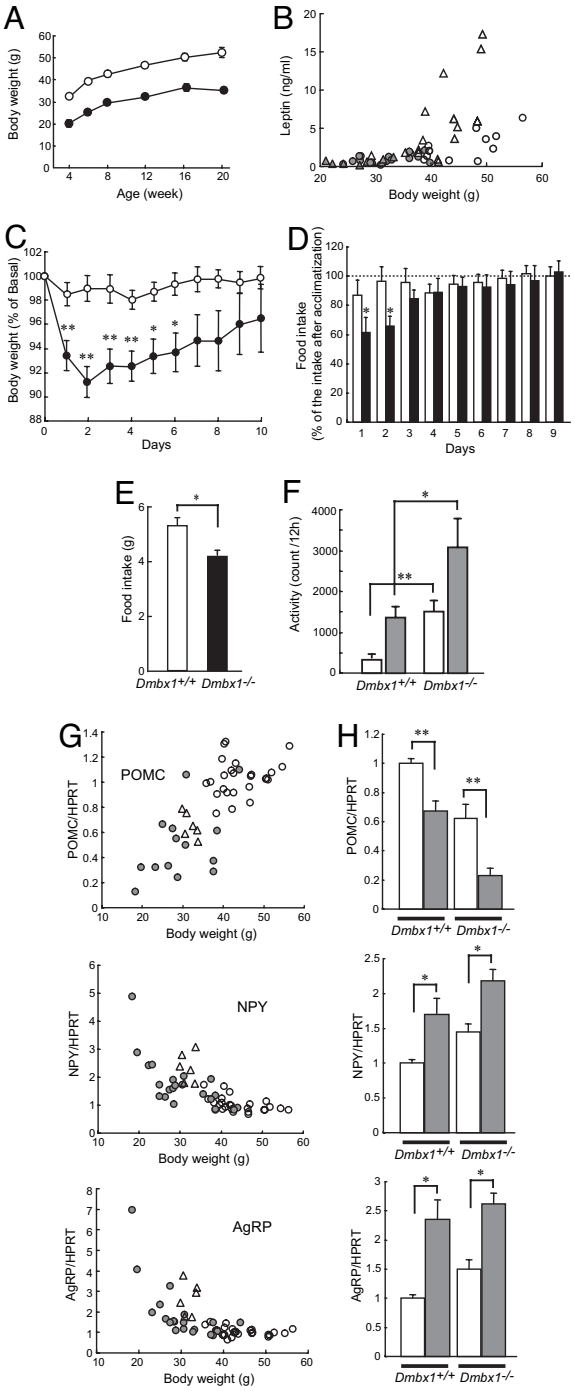

Fig. 1. Phenotype of *Dmbx1*$^{-/-}$ mice. (*A*) Growth curves of *Dmbx1*$^{+/+}$ (white circles) and *Dmbx1*$^{-/-}$ (black circles) mice. The data are from 7–11 male mice for each time point. (*B*) Relationship between body weight and serum leptin levels in *Dmbx1*$^{+/+}$ mice (white circles, male; white triangles, female) and *Dmbx1*$^{-/-}$ mice (gray circles, male; gray triangles, female) at 16 wk of age. (*C*) Changes in body weight after isolation. Body weight of *Dmbx1*$^{+/+}$ (white circles; $n = 12$) and *Dmbx1*$^{-/-}$ (black circles; $n = 11$) female mice are expressed as a percentage of those on the day of isolation (day 0). *, $P < 0.05$; **, $P < 0.005$ (vs. *Dmbx1*$^{+/+}$). (*D*) Changes in food intake after isolation. Food intake of *Dmbx1*$^{+/+}$ female mice (white columns; $n = 12$) and *Dmbx1*$^{-/-}$ female mice (black columns; $n = 11$) is expressed as a percentage of the average food intake after a 4-wk acclimatization period. *, $P < 0.05$ (vs. *Dmbx1*$^{+/+}$). (*C* and *D*) The data are from female mice at 24–28 wk of age. (*E*) Daily food intake after the acclimatizing period of *Dmbx1*$^{+/+}$ male mice (white column; $n = 16$) and *Dmbx1*$^{-/-}$ male mice (black column; $n = 20$) at 24–28 wk of age. *, $P < 0.002$. (*F*) Locomotor activity. Spontaneous locomotor activity of *Dmbx1*$^{+/+}$ ($n = 9$) and *Dmbx1*$^{-/-}$ ($n = 7$) male mice at 28–32 wk of age is expressed as the count of infrared-beam splits during a 12-h time period during the light phase (0800–2000 hours; white columns) and dark phase (2000–0800 hours; gray columns). *, $P < 0.05$; **, $P < 0.005$ (vs. *Dmbx1*$^{+/+}$). (*G*) mRNA expressions of neuropeptides in the hypothalamus. Relationship between body weight and mRNA expression levels in the hypothalamus of *Dmbx1*$^{+/+}$ mice fed ad libitum (white circles), food-restricted *Dmbx1*$^{+/+}$ mice (white triangles), and *Dmbx1*$^{-/-}$ mice (gray circles). (*H*) Changes in mRNA expression levels in the hypothalamus by fasting ($n = 6$–12). *, $P < 0.05$; **, $P < 0.005$ (vs. *Dmbx1*$^{+/+}$). (*G* and *H*) The data are from female mice at 28–32 wk of age.

of *Dmbx1*$^{+/+}$ mice during the first 6 days of isolation (Fig. 1*C*). The food intake by *Dmbx1*$^{-/-}$ mice during the first 2 days of isolation was significantly decreased by 40% compared with the average food intake after 4 wk of the acclimatization period, whereas no significant decrease in food intake was found in *Dmbx1*$^{+/+}$ mice (Fig. 1*D*).

Food intake of individually housed male *Dmbx1*$^{-/-}$ mice also was significantly reduced compared with that of *Dmbx1*$^{+/+}$ mice (Fig. 1*E*). We also compared the locomotor activities of *Dmbx1*$^{+/+}$ and *Dmbx1*$^{-/-}$ mice under unstressed, freely moving conditions (Fig. 1*F*). Measurement of locomotor activity, as assessed by the count of infrared-beam breaks, revealed that *Dmbx1*$^{-/-}$ mice were markedly hyperactive both in the light phase (Fig. 1*F*, white columns) and dark phase (Fig. 1*F*, gray columns), suggesting that hyperactivity contributes to the development of leanness in *Dmbx1*$^{-/-}$ mice.

Normal Regulation of Neuropeptide Expression in the Hypothalamus of *Dmbx1*$^{-/-}$ Mice. The leanness associated with hypophagia and hyperactivity in *Dmbx1*$^{-/-}$ mice suggested abnormality in the maintenance of energy homeostasis. Therefore, the mRNA expression of neuropeptides in the hypothalamus was examined by real time RT-PCR analysis. mRNA expression of *Pomc* was decreased, whereas mRNA expression of *Npy* and *Agrp* was increased in *Dmbx1*$^{-/-}$ mice compared with *Dmbx1*$^{+/+}$ mice (Fig. 1*G*). When each value of the *Dmbx1*$^{-/-}$ mouse was plotted with the body weight, there was positive correlation with the body weight in POMC and negative correlations in NPY and AgRP (Fig. 1*G*, gray circles). Similar correlations also were found in *Dmbx1*$^{+/+}$ mice fed ad libitum (Fig. 1*G*, white circles) and *Dmbx1*$^{+/+}$ mice with reduced body weight by food restriction (Fig. 1*G*, white triangles), suggesting that the differences in expression of these neuropeptides in *Dmbx1*$^{-/-}$ mice are not primarily caused by the disruption of Dmbx1 function but are secondary to the leanness of *Dmbx1*$^{-/-}$ mice. We also measured changes in the expression of *Pomc*, *Npy*, and *Agrp* induced by 48-h food deprivation. Fasting decreased *Pomc* expression and increased *Npy* and *Agrp* expressions in both *Dmbx1*$^{+/+}$ and *Dmbx1*$^{-/-}$ mice (Fig. 1*H*), indicating that the regulation of mRNA expression of these neuropeptides during fasting is intact in *Dmbx1*$^{-/-}$ mice and that the expression profile of POMC, NPY, and AgRP in the hypothalamus of *Dmbx1*$^{-/-}$ mice reflects their poor nutritional status.

Preserved Leptin Action in *Dmbx1*$^{-/-}$ Mice. Feeding and peripheral energy expenditure are regulated by both anorexigenic and orexigenic signaling. We evaluated the leptin-mediated anorexigenic response by cross-breeding *Dmbx1*$^{-/-}$ mice with leptin-deficient *Lep*$^{ob/ob}$ mice. The body weight and blood glucose levels of double-knockout (*Dmbx1*$^{-/-}$;*Lep*$^{ob/ob}$) mice were lower than the body weight and blood glucose levels in *Lep*$^{ob/ob}$ mice but were significantly higher than in *Dmbx1*$^{-/-}$ mice (SI Fig. 7 *A* and *B*). In addition, *Dmbx1*$^{-/-}$;*Lep*$^{ob/ob}$ mice exhibited markedly increased serum insulin levels compared with *Dmbx1*$^{-/-}$ mice (SI Fig. 7*C*).

Abolishment of Pleiotropic Effects of Lethal Yellow (A^y) Mutation by Dmbx1 Deficiency. Because leptin simultaneously stimulates anorexigenic signaling and inhibits orexigenic signaling, both are affected in $Lep^{ob/ob}$ mice (1, 3, 4). To determine which signaling is operative in $Dmbx1^{-/-}$ mice, we also crossed $Dmbx1^{-/-}$ mice with lethal yellow (A^y/a) mice, in which the ectopic expression of agouti protein blocks α-MSH signaling via MC4R, resulting in marked obesity and diabetes mellitus associated with hyperphagia and insulin resistance (19). Although A^y/a mice exhibited marked obesity after 12 wk of age, the body weight of the double mutant ($Dmbx1^{-/-}$;A^y/a) mice was not significantly different from that of $Dmbx1^{-/-}$ mice in both male (Fig. 2 *A* and *B*) and female (data not shown) mice, indicating that there is essentially no sex difference in the phenotype of $Dmbx1^{-/-}$ mice. In addition to late-onset obesity, male A^y/a mice developed diabetes mellitus, but hyperglycemia did not occur in $Dmbx1^{-/-}$;A^y/a mice (Fig. 2*C*). Moreover, serum insulin levels were markedly elevated in A^y/a mice, whereas those of $Dmbx1^{-/-}$;A^y/a mice were similar to those of $Dmbx1^{-/-}$ mice (Fig. 2*D*). The tissue weight of retroperitoneal adipose tissue in $Dmbx1^{-/-}$ mice was significantly decreased, whereas that in A^y/a mice was markedly increased compared with $Dmbx1^{+/+}$ mice (Fig. 2*E*). The weight of adipose tissue in $Dmbx1^{-/-}$;A^y/a mice was between that of $Dmbx1^{-/-}$ and $Dmbx1^{+/+}$ mice. The tissue weight of the liver of A^y/a mice was significantly increased compared with that of $Dmbx1^{+/+}$ mice, whereas that of $Dmbx1^{-/-}$;A^y/a mice was similar to that of $Dmbx1^{-/-}$ mice (Fig. 2*F*). Histological examination of liver revealed that A^y/a mice developed liver steatosis, a fatty degeneration in hepatocytes, but steatotic change was not found in $Dmbx1^{-/-}$;A^y/a mice (SI Fig. 8). Similarly, the food intake of A^y/a mice was significantly increased, whereas that of $Dmbx1^{-/-}$;A^y/a mice did not differ from that of $Dmbx1^{-/-}$ mice (Fig. 2*G*). The locomotor activity of $Dmbx1^{-/-}$;A^y/a mice was significantly increased to a level similar to that of $Dmbx1^{-/-}$ mice (Fig. 2*H*). These findings demonstrate that Dmbx1 deficiency can rescue the pleiotropic effects of the lethal yellow (A^y) mutation in A^y/a mice, including hyperphagia, obesity, hyperglycemia, and insulin resistance.

Lack of Orexigenic Effect of AgRP in $Dmbx1^{-/-}$ Mice. We evaluated the leptin-mediated anorexigenic response by examining leptin-induced STAT3 phosphorylation (20) in the hypothalamus and by measuring food intake in $Dmbx1^{-/-}$ mice. Administration (i.p.) of leptin (2 mg/kg) induced STAT3 phosphorylation in both $Dmbx1^{+/+}$ and $Dmbx1^{-/-}$ mice (SI Fig. 9 and *SI Materials and Methods*). In addition, the food intake was suppressed by intracerebroventricularly (i.c.v.) administered leptin (10 nmol) in both $Dmbx1^{+/+}$ and $Dmbx1^{-/-}$ mice (Fig. 3*A*), indicating that the anorexigenic effect of leptin is retained in $Dmbx1^{-/-}$ mice. We also evaluated regulation of feeding by neuropeptides in $Dmbx1^{+/+}$ and $Dmbx1^{-/-}$ mice. For this purpose, NPY, AgRP, or the melanocortin receptor antagonist SHU9119 (21) or the agonist melanotan-II (MT-II) (22) was administered i.c.v., after which food intake was measured (Fig. 3 *B–F*). In both genotypes, NPY (0.5 nmol) increased the food intake significantly (Fig. 3*B*). Administration of either SHU9119 or AgRP nearly doubled food intake by $Dmbx1^{+/+}$ mice during the first 6 h (Fig. 3*C*), the effects persisting for 24 h (Fig. 3*D*) and for 3 days (Fig. 3*E*) in the case of AgRP. By contrast, $Dmbx1^{-/-}$ mice showed an increase in feeding in response to either SHU9119 or AgRP at 6 h (Fig. 3*C*) that did not persist to 24 h (Fig. 3*D*). In fact, administration of AgRP was found to inhibit food intake by $Dmbx1^{-/-}$ mice at 24 h and at 3 days (Fig. 3 *D* and *E*). We also examined the effect of MT-II on feeding. The administration of MT-II (0.1 nmol) suppressed the food intake of both $Dmbx1^{+/+}$ and $Dmbx1^{-/-}$ mice (Fig. 3*F*), suggesting that the anorexic effect of melanocortin through MC4R remains intact in $Dmbx1^{-/-}$ mice.

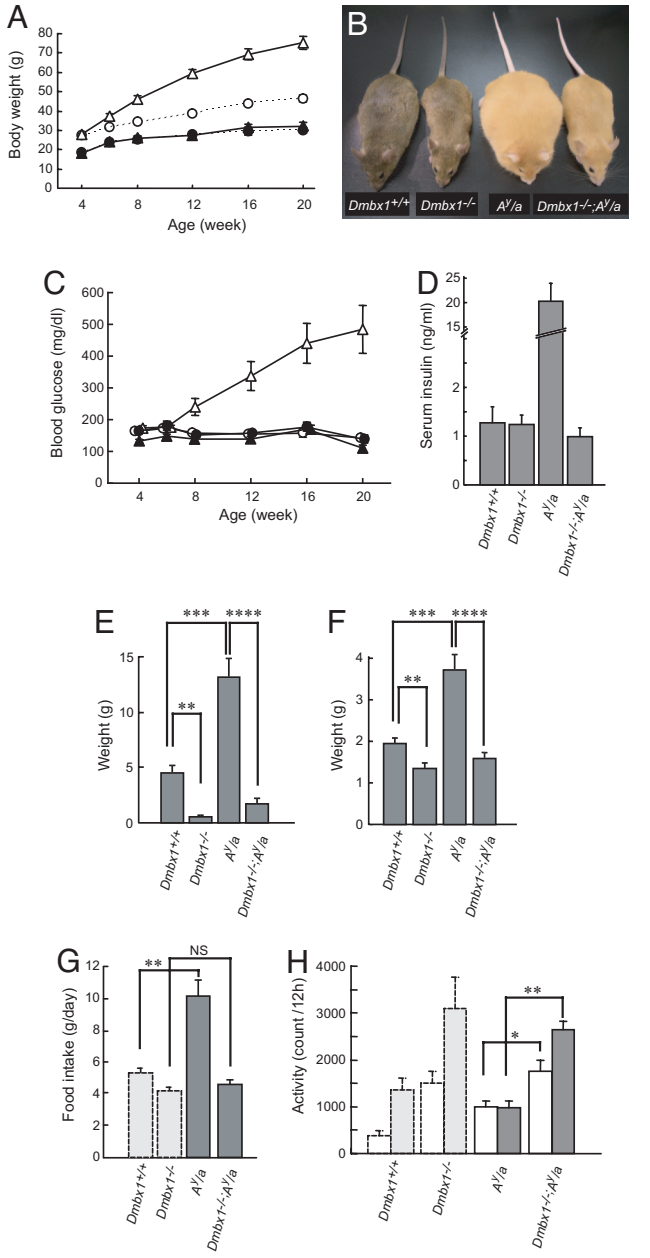

Fig. 2. Phenotype of $Dmbx1^{-/-}$;A^y/a mice. (*A*) Growth curves of $Dmbx1^{+/+}$ (white circles), $Dmbx1^{-/-}$ (black circles), A^y/a (white triangles), and $Dmbx1^{-/-}$;A^y/a (black triangles) male mice. The dotted lines for $Dmbx1^{+/+}$ and $Dmbx1^{-/-}$ mice are the same as in Fig. 1*A*. (*B*) Representative photographs of each genotype. (*C*) Blood glucose levels of $Dmbx1^{+/+}$ (white circles), $Dmbx1^{-/-}$ (black circles), A^y/a (white triangles), and $Dmbx1^{-/-}$;A^y/a (black triangles) male mice. (*D*) Serum insulin levels in mice at 16 wk of age. The data are from 7–11 male mice for each genotype. (*E* and *F*) Tissue weight [retroperitoneal fat (*E*) and liver (*F*)] of $Dmbx1^{+/+}$ ($n = 7$), $Dmbx1^{-/-}$ ($n = 6$), A^y/a ($n = 7$), and $Dmbx1^{-/-}$;A^y/a male mice ($n = 6$). (*G*) Daily food intake of A^y/a ($n = 8$) and $Dmbx1^{-/-}$;A^y/a ($n = 12$) male mice at 28–32 wk of age. (*H*) Locomotor activity. Spontaneous locomotor activity of each genotype is shown. The data are from 7–9 male mice at 28–32 wk of age for each genotype. (*G* and *H*) The results of $Dmbx1^{+/+}$ and $Dmbx1^{-/-}$ mice (light gray columns, same as in Fig. 1 *E* and *F*) also are shown for comparison. *, $P < 0.05$; **, $P < 0.005$; ***, $P < 0.001$; ****, $P < 0.00005$; and NS, not significant.

Expression of Dmbx1 in Brain Stem of Embryo. To determine the region of the brain in which Dmbx1 influences the regulation of energy balance, we performed *in situ* hybridization experiments

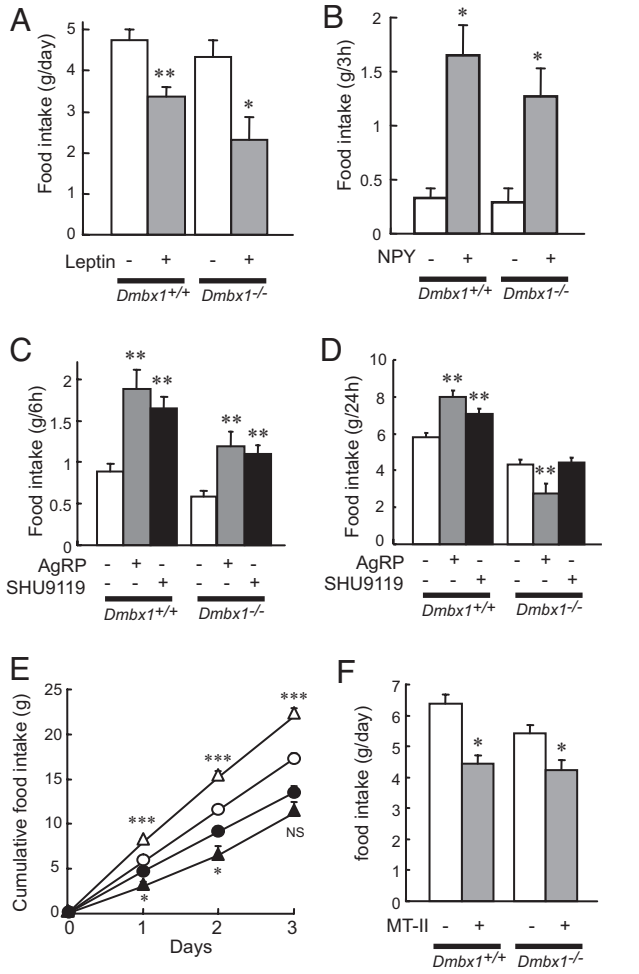

Fig. 3. Changes in food intake by i.c.v. administration of leptin, NPY, SHU9119, AgRP, and MT-II. (*A* and *B*) The changes in the food intake of *Dmbx1*$^{+/+}$ ($n = 5$) and *Dmbx1*$^{-/-}$ ($n = 5$–7) mice by leptin (*A*; gray columns) or NPY (*B*; gray columns) and vehicle (white columns) are shown. (*C* and *D*) Cumulative food intake for 6 h (*C*) or 24 h (*D*) for *Dmbx1*$^{+/+}$ ($n = 7$–19) and *Dmbx1*$^{-/-}$ ($n = 6$–14) mice by AgRP (gray columns), SHU9119 (black columns), or vehicle (white columns) is shown. (*E*) Cumulative food intake for 3 days for *Dmbx1*$^{+/+}$ mice (white circles and triangles, $n = 12$–19) and *Dmbx1*$^{-/-}$ mice (black circles and triangles, $n = 14$–18) by AgRP (triangles) or vehicle (circles) is shown. (*F*) Cumulative food intake for 24 h for *Dmbx1*$^{+/+}$ ($n = 7$) and *Dmbx1*$^{-/-}$ ($n = 7$) mice by MT-II (gray columns) or vehicle (white columns) is shown. *, $P < 0.05$; **, $P < 0.005$; ***. $P < 0.0005$; and NS, not significant (vs. vehicle administration).

of fetal brain of wild-type mice. Although mouse *Dmbx1* is expressed in the anterior region (diencephalon and mesencephalon) of the brain at embryonic day (E)10.5 and E11.5 (diencephalon mesencephalon homeobox 1), we found that *Dmbx1* is expressed in a subset of neurons in the mesencephalon, metencephalon, and myelencephalon at the stages later than E11.5. The *in situ* hybridization experiment using E15.5 mouse embryos (Fig. 4) revealed that *Dmbx1* is expressed in parabrachial nuclei, including the lateral parabrachial nucleus (Fig. 4 *A* and *B*) and superior colliculus in the mesencephalon (data not shown) and rostral nucleus of the tractus solitarius (NTS) (Fig. 4 *C* and *D*), dorsal motor nucleus of the vagus, and reticular nucleus in the medulla oblongata (Fig. 4 *E* and *F*) but not in the hypothalamus. POMC neurons in the arcuate nucleus are known to project to lateral parabrachial nucleus, rostral NTS, dorsal motor nucleus of the vagus, and reticular nucleus (5), and MC4R is abundantly expressed in superior colliculus in addition to lateral parabrachial nucleus, NTS, dorsal motor nucleus of the vagus, and reticular nucleus (23). Thus, *Dmbx1* is expressed at high levels in the fetal brain regions that develop neurons receiving melanocortin signaling in the adult brainstem. The transcripts of *Dmbx1* in all of the regions mentioned above have almost disappeared in the brain of E17.5 fetuses.

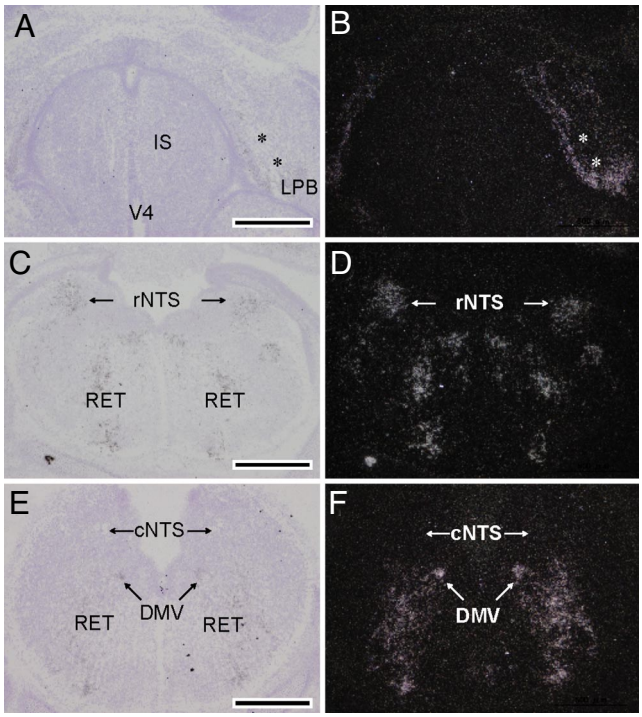

Fig. 4. *In situ* hybridization analysis of Dmbx1 mRNA in the mesencephalon, pons, and medulla of E15.5 mouse fetuses. The lateral parabrachial nucleus (LPB) around the superior cerebellar peduncle (asterisks in *A* and *B*) is strongly labeled with silver grains. IS, isthmus; V4, fourth ventricle. The rostral NTS (rNTS) shows signals, whereas the caudal NTS (cNTS) does not (*C*–*F*). (*E* and *F*) Significant signals in the medulla also are distributed in the dorsal motor nucleus of vagus (DMV) and the reticular nucleus (RET). *B*, *D*, and *F* are dark-field images of *A*, *C*, and *E*, respectively. (Scale bars, 500 μm.)

Morphological Analysis of Adult Brain of *Dmbx1*$^{+/+}$ Mice and *Dmbx1*$^{-/-}$ Mice. Immunohistochemical analyses revealed no abnormalities in either the fiber densities of AgRP neurons and POMC neurons in the hypothalamus and the dorsal pons (including parabrachial nuclei) (SI Fig. 10) or in the abundance of tyrosine hydroxylase-positive neurons in the hypothalamus and the ventral tegmental area (SI Fig. 11). We also found no spongiform degeneration resembling that in attractin/mahogany or mahoganoid mutants (SI Fig. 12) (24).

Discussion

Dmbx1$^{-/-}$ mice exhibit hypophagia and hyperactivity despite severe leanness, suggesting abnormality in the maintenance of energy homeostasis. However, normal regulation of POMC, AgRP, and NPY expression in the hypothalamus of *Dmbx1*$^{-/-}$ mice indicates that a defect in the regulation of food intake and energy expenditure in *Dmbx1*$^{-/-}$ mice occurs downstream from transcriptional regulation of these neuropeptides. Because inactivation of the leptin gene in *Dmbx1*$^{-/-}$ mice induced body weight gain and insulin resistance compared with *Dmbx1*$^{-/-}$ mice, the effects of leptin are largely preserved in *Dmbx1*$^{-/-}$ mice. These results are in accord with the normal STAT3 phosphorylation and normal anorexigenic response to leptin found in *Dmbx1*$^{-/-}$ mice.

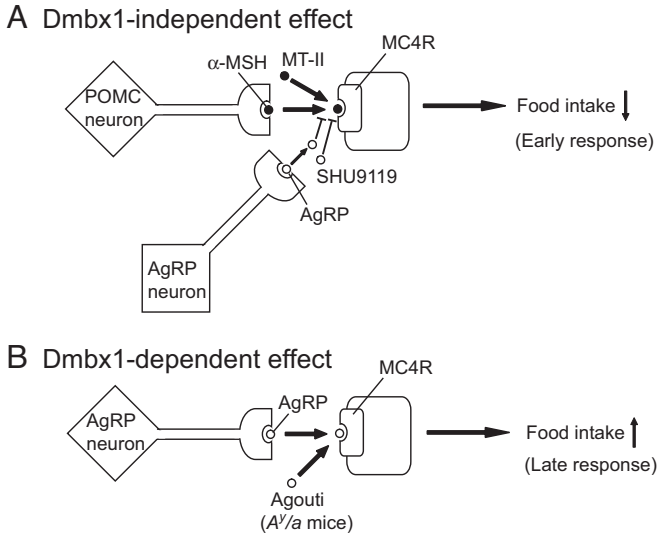

Fig. 5. Dmbx1-independent and Dmbx1-dependent effects of AgRP on food intake. See the text for details.

Leptin not only activates the anorexigenic response through melanocortin signaling, it also inhibits the orexigenic response mediated by NPY and AgRP signaling. To examine the orexigenic response to AgRP signaling of *Dmbx1*$^{-/-}$ mice, they were bred with *A*^{y}*/a* mice, in which ectopically expressed agouti protein blocks the anorexigenic pathway, promoting obesity, hyperglycemia, and hyperinsulinemia (19). Interestingly, the phenotype of *A*^{y}*/a* mice was almost completely abolished by genetic disruption of *Dmbx1*. The increased retroperitoneal fat deposit, insulin resistance, steatosis of the liver, and hyperphagia in *A*^{y}*/a* mice were all restored in the absence of Dmbx1, clearly indicating that AgRP action is impaired in *Dmbx1*$^{-/-}$ mice.

AgRP promotes food intake and positive energy balance, when assessed by its transgenic overexpression (25) or i.c.v. administration (26). Recent studies of mice in which AgRP neurons were postnatally ablated have shown that AgRP neurons are essential for regulating food intake and weight gain (7–10). In addition, in contrast to the initial study (6), *Agrp*$^{-/-}$ mice were found to exhibit leanness with hyperactivity as they become older (11). Because the leanness of *Dmbx1*$^{-/-}$ mice was more severe than in *Agrp*$^{-/-}$ mice, various factors other than unresponsiveness to AgRP are involved in the development of leanness in *Dmbx1*$^{-/-}$ mice.

It has been reported that c-Fos expression patterns in the brain by AgRP administration differ in the early phase (2 h) and the late phase (24 h) (27). In *Dmbx1*$^{-/-}$ mice, the orexigenic effect of AgRP was observed at 6 h but was abolished at 24 h, suggesting that AgRP elicits two distinct effects: Dmbx1-independent and Dmbx1-dependent effects, as shown in Fig. 5. Because the anorexic effect of MT-II remained unaffected in *Dmbx1*$^{-/-}$ mice, the α-MSH/MC4R signaling is operative in a Dmbx1-independent manner. In accord with this finding, blocking the signaling with SHU9119 or AgRP significantly increased the food intake both in *Dmbx1*$^{+/+}$ and *Dmbx1*$^{-/-}$ mice at 6 h. Although the orexigenic effect of SHU9119 became smaller at 24 h after the administration, the effect of AgRP still remained at 1–3 days after the administration. Because this late effect of AgRP on feeding was completely abolished in *Dmbx1*$^{-/-}$ mice, the effect likely depends on Dmbx1 function. In addition, the phenotype of *A*^{y}*/a* mice almost completely disappeared by genetic disruption of Dmbx1, indicating that Dmbx1-dependent signaling is important for the regulation of adiposity, satiety, and the insulin-resistant state by AgRP. In addition to the competitive blockade of α-MSH at MC4R, AgRP also is shown to act as an inverse agonist at MC4R (28). Thus, the Dmbx1-dependent effect of AgRP might well be mediated by this mechanism.

Dmbx1 was identified independently by several groups, and its expression pattern in mouse embryo has been reported in refs. 12–15. These studies have shown that, although Dmbx1 is expressed abundantly and diffusely in the mantle layer of the diencephalon and mesencephalon at E10.5, the expression of Dmbx1 at later stages is restricted to several regions, including brainstem nuclei (13, 14). By analyzing in detail the expression pattern of fetal brain at later developmental stages, we found that the *Dmbx1* gene also is expressed in the brain nuclei that give rise to the neurons receiving melanocortin signaling in the brainstem at E15.5, but the *Dmbx1* gene almost disappears at E17.5. There were no apparent abnormalities in adult brain regions of *Dmbx1*$^{-/-}$ mice corresponding to embryonic (E15.5) brain regions in which Dmbx1 is expressed. These expression profiles of Dmbx1 suggest that Dmbx1 plays a role in the maintenance of energy homeostasis by contributing to the development of neurons that are downstream targets of NPY/AgRP neurons and/or POMC neurons.

We also found that isolation of *Dmbx1*$^{-/-}$ mice from their cohabitants significantly decreased food intake, resulting in a transient but significant weight loss. Isolation is known to cause self-induced weight loss in rodents and has been proposed as an experimental method to study the pathophysiology of anorexia by stress (29). In addition, *Dmbx1*$^{-/-}$ mice exhibit markedly increased locomotion activity, which likely contributes to the development of leanness. These features of *Dmbx1*$^{-/-}$ mice are similar to those of restricting anorexia nervosa (RAN) in humans (30). RAN is a rare and severe subtype of anorexia nervosa and differs from binge-eating/purging anorexia nervosa (a more common subtype of anorexia nervosa) in that RAN patients exhibit persistent hypophagia without binge eating or purging behavior and have a stronger genetic predisposition (31). Considering that a susceptibility gene for RAN has been mapped near *DMBX1* on human chromosome 1p (only a 5.3-megabase distance to D1S3721, the marker for RAN) (31, 32), it is of interest to learn whether genetic alterations of *DMBX1* are associated with RAN in these families.

Materials and Methods

Animals. Dmbx1-deficient (*Dmbx1*$^{-/-}$) mice were generated as shown in SI Fig. 13 and as described in *SI Materials and Methods*.

Feeding Behavior and Activity. Feeding behavior and locomoter activities were monitored as described in *SI Materials and Methods.*

Real-Time PCR Analysis. Real-time quantitative RT-PCR was performed by *Taq*Man probes (PerkinElmer, Boston, MA and Applied Biosystems, Foster City, CA) by using a PRIZM 7000 apparatus as described in *SI Materials and Methods*. The amount of *Pomc*, *Npy*, or *Agrp* mRNA was normalized by that of hypoxanthine–guanine phosphoribosyltransferase (*Hprt*) mRNA and expressed relative to that of *Dmbx1*$^{+/+}$ mice fed ad libitum.

Measurements of Food Intake by i.c.v. Administration of Compounds. After acclimatization to single-housing, mice were implanted with a stainless catheter in the lateral ventricle and were challenged by orexigenic and anorexigenic compounds. The mice eating ad libitum were administrated i.c.v. with 10 nmol of mouse leptin, 0.5 nmol of human/rat NPY (Peptide Institute, Osaka, Japan), 1 nmol of SHU9119 (Sigma, St. Louis, MO), 0.5 nmol of human AgRP$_{86–132}$ (Peptide Institute), or 0.1 nmol of MT-II (Phoenix Pharmaceuticals Burlingame, CA) at 0900 hours. As a control, vehicle (saline) was administrated. The

cumulative food intake was measured at the time points indicated in Fig. 3. The food used was normal mouse chow, CE-2 (Japan Clea, Tokyo, Japan).

***In Situ* Hybridization.** *In situ* hybridization of *Dmbx1* was performed as described in ref. 33. Nonoverlapping antisense oligonucleotide probes (45 mer in length) were designed to be complementary to nucleotides 401–445 and 984-1028 (NM_130865). The hybridization using two ^{33}P-labeled probes exhibited consistent labeling in all of the regions.

Statistical Analysis. Results are expressed as means ± SEM. Comparisons between groups were made by unpaired, two-tailed Student *t* test. $P < 0.05$ was considered to be statistically significant.

We thank H. Koseki for support in generating the knockout mice; A. Saraya, Y. Zhang, and K. Kimura for involvement in the initial stage of the study; M. Schwartz for helpful suggestions for the study; and R. Palmiter for valuable discussion and critical reading of the paper. This work was supported by a Grant-in-Aid for Specially Promoted Research and for Scientific Research from the Ministry of Education, Science, Sports, Culture, and Technology, by a Grant-in Aid for Core Research for Evolutional Science and Technology, and by a grant from the Setsuro Fujii Memorial Osaka Foundation of Fundamental Medical Research.

1. Schwartz MW, Woods SC, Porte D, Jr, Seeley RJ, Baskin DG (2000) *Nature* 404:661–671.
2. Alquier T, Kahn BB (2004) *Endocrinology* 145:4022–4024.
3. Flier JS (2004) *Cell* 116:337–350.
4. Seeley RJ, Woods SC (2003) *Nat Rev Neurosci* 4:901–909.
5. Cone RD (2005) *Nat Neurosci* 8:571–578.
6. Qian S, Chen H, Weingarth D, Trumbauer ME, Novi DE, Guan X, Yu H, Shen Z, Feng Y, Frazier E, *et al.* (2002) *Mol Cell Biol* 22:5027–5035.
7. Luquet S, Perez FA, Hnasko TS, Palmiter RD (2005) *Science* 310:683–685.
8. Gropp E, Shanabrough M, Borok E, Xu AW, Janoschek R, Buch T, Plum L, Balthasar N, Hampel B, Waisman A, *et al.* (2005) *Nat Neurosci* 8:1289–1291.
9. Bewick GA, Gardiner JV, Dhillo WS, Kent AS, White NE, Webster Z, Ghatei MA, Bloom SR (2005) *FASEB J* 19:1680–1682.
10. Xu AW, Kaelin CB, Morton GJ, Ogimoto K, Stanhope K, Graham J, Baskin DG, Havel P, Schwartz MW, Barsh GS (2005) *PLoS Biol* 3:2168–2176.
11. Wortley KE, Anderson KD, Yasenchak J, Murphy A, Valenzuela D, Diano S, Yancopoulos GD, Wiegand SJ, Sleeman MW (2005) *Cell Metab* 2:421–427.
12. Ohtoshi A, Nishijima I, Justice MJ, Behringer RR (2002) *Mech Dev* 110:241–244.
13. Zhang Y, Miki T, Iwanaga T, Koseki Y, Okuno M, Sunaga Y, Ozaki N, Yano H, Koseki H, Seino S (2002) *J Biol Chem* 277:28065–28069.
14. Takahashi T, Holland PW, Cohn MJ, Shimizu K, Kurokawa M, Hirai H (2002) *Dev Genes Evol* 212:293–297.
15. Gogoi RN, Schubert FR, Martinez-Barbera JP, Acampora D, Simeone A, Lumsden A (2002) *Mech Dev* 114:213–217.
16. Broccoli V, Colombo E, Cossu G (2002) *Mech Dev* 114:219–223.
17. Ohtoshi A, Behringer RR (2004) *Mol Cell Biol* 24:7548–7558.
18. Considine RV, Sinha MK, Heiman ML, Kriauciunas A, Stephens TW, Nyce MR, Ohannesian JP, Marco CC, McKee LJ, Bauer TL, *et al.* (1996) *N Engl J Med* 334:292–295.
19. Flier JS (2006) *Cell Metab* 3:83–85.
20. Vaisse C, Halaas JL, Horvath CM, Darnell JE, Jr, Stoffel M, Friedman JM (1996) *Nat Genet* 14:95–97.
21. Fan W, Boston BA, Kesterson RA, Hruby VJ, Cone RD (1997) *Nature* 385:165–168.
22. Marsh DJ, Hollopeter G, Huszar D, Laufer R, Yagaloff KA, Fisher SL, Burn P, Palmiter RD (1999) *Nat Genet* 21:119–122.
23. Kishi T, Aschkenasi CJ, Lee CE, Mountjoy KG, Saper CB, Elmquist JK (2003) *J Comp Neurol* 457:213–235.
24. He L, Lu XY, Jolly AF, Eldridge AG, Watson SJ, Jackson PK, Barsh GS, Gunn TM (2003) *Science* 299:710–712.
25. Ollmann MM, Wilson BD, Yang YK, Kerns JA, Chen Y, Gantz I, Barsh GS (1997) *Science* 278:135–138.
26. Rossi M, Kim MS, Morgan DG, Small CJ, Edwards CM, Sunter D, Abusnana S, Goldstone AP, Russell SH, Stanley SA, *et al.* (1998) *Endocrinology* 139:4428–4431.
27. Hagan MM, Rushing PA, Pritchard LM, Schwartz MW, Strack AM, Van Der Ploeg LH, Woods SC, Seeley RJ (2000) *Am J Physiol* 279:R47–R52.
28. Smith MA, Hisadome K, Al-Qassab H, Heffron H, Withers DJ, Ashford ML (2007) *J Physiol* 578:425–438.
29. van Leeuwen SD, Bonne OB, Avraham Y, Berry EM (1997) *Physiol Behav* 62:77–81.
30. Fairburn CG, Harrison PJ (2003) *Lancet* 361:407–416.
31. Devlin B, Bacanu SA, Klump KL, Bulik CM, Fichter MM, Halmi KA, Kaplan AS, Strober M, Treasure J, Woodside DB, *et al.* (2002) *Hum Mol Genet* 11:689–696.
32. Grice DE, Halmi KA, Fichter MM, Strober M, Woodside DB, Treasure JT, Kaplan AS, Magistretti PJ, Goldman D, Bulik CM, *et al.* (2002) *Am J Hum Genet* 70:787–792.
33. Tanaka J, Murate M, Wang CZ, Seino S, Iwanaga T (1996) *Arch Histol Cytol* 59:485–490.